Organic Ionic Plastic Crystal-Based Composite Electrolyte with Surface Enhanced Ion Transport and Its Use in All-Solid-State Lithium Batteries

*Xiaoen Wang, Haijin Zhu, George W. Greene, Yundong Zhou, Masahiro Yoshizawa-Fujita, Yukari Miyachi, Michel Armand, Maria Forsyth, Jennifer M. Pringle, and Patrick C. Howlett**

Solid-state electrolytes have been identified as one of the most attractive materials for the fabrication of reliable and safe lithium batteries. This work demonstrates a facile strategy to prepare highly conductive organic ionic plastic crystal (OIPC) composites by combination of a low weight fraction of Li^+ doped OIPC (*N*-ethyl-*N*-methylpyrrolidinium bis(fluorosulfonyl)amide, [C_2mpyr][FSI]) with commercial poly(vinylidene difluoride) (PVDF) powder. Benefiting from the enhancement of lithium ion dynamics, as evidenced by the solid-state NMR measurements, the composite electrolyte shows an order of magnitude higher conductivity than that of the bulk material. Lithium metal/$LiFePO_4$ cells incorporating the prepared composite electrolytes show impressively high specific capacity and good cycling stability (99.8% coulombic efficiency after 1200 cycles at 2 C, room temperature), which is the first demonstration of long-term cycling performance at such high rate for an OIPC-based electrolyte. The high voltage cathode, $LiCo_{1/3}Ni_{1/3}Mn_{1/3}O_2$ was tested and good rate performance and stable capacities have been achieved.

With the motivation of developing more reliable and safer lithium batteries, solid electrolytes have received increasing attention as they can reduce solvent leakage problems and have the ability to suppress lithium dendrite growth.[1] As a result of the good mechanical stability and flexibility, polymer electrolytes such as single ion conducting polymers[2] or polymer–salt systems,[3] have been widely investigated. However, such systems suffer from low ionic conductivity due to limited dissociation of the lithium ions from the polymer backbone or from the anion of lithium salts.[3] The addition of plasticizers has been shown to be an effective strategy to improve the conductivity of polymer electrolytes.[4] However, the subsequent mechanical deterioration (e.g., decrease of shear modulus) remains an issue in pursuit of long lived lithium batteries. Another group of solid ion conducting materials, inorganic Li-fast ion conductors,[5] has displayed impressively high lithium conductivity, but their inherent brittleness hinders their broad application. Thus, achieving a solid electrolyte with high conductivity and suitable mechanical properties (i.e., mechanically strong but not rigid) is highly desirable for practical development of high performance all-solid-state lithium ion batteries.

Organic ionic plastic crystals (OIPCs), structural analogues of ionic liquids but in solid form at room temperature (RT), have received considerable attention because of their attractive combination of chemical/electrochemical stability, high thermal stability, and plastic mechanical properties,[6] which makes them promising candidates for application in electrochemical devices.[7] OIPCs are composed of small organic cations and anions with short-range molecular rotational/orientational motions and long-range crystalline structures.[6b] These structural features can give OIPCs several unique properties, such as multiple solid–solid phase transitions and the capability of forming a "plastic" or disordered phase, which can greatly improve the electrolyte/electrode interfacial contact and, most importantly, facilitate ion diffusion. For instance, the ionic conductivity of the previously reported OIPC diethyl(methyl)(isobutyl)phosphonium hexafluorophosphate ([$P_{1,2,2,4}$][PF_6]) is around 10^{-3} S cm^{-1} in phase I (the plastic phase before melting, in this case spanning between 120 and 150 °C), which is around five orders of magnitude higher than the conductivity in the room temperature phase.[8] However, the plastic phase transition temperature of this OIPC is relatively high, making it less suitable for room temperature or medium temperature (e.g., 30–80 °C) applications. Recently, an attractive

Dr. X. Wang, Dr. H. Zhu, Dr. G. W. Greene, Y. Zhou, Prof. M. Forsyth, Dr. J. M. Pringle, Dr. P. C. Howlett
Institute for Frontier Materials (IFM)
Deakin University
Waurn Ponds Campus, Geelong, VIC 3216, Australia
E-mail: patrick.howlett@deakin.edu.au
Dr. M. Yoshizawa-Fujita, Y. Miyachi
Department of Materials and Life Sciences
Sophia University
7-1 Kioi-cho, Chiyoda-ku, Tokyo 102-8554, Japan
Prof. M. Armand
Alava Technology Park
CIC Energigune
C/Albert Einstein 48, 4801510 MIÑANO, Álava, Spain

DOI: 10.1002/admt.201700046

OIPC, *N*-ethyl-*N*-methylpyrrolidinium bis(fluorosulfonyl)amide ([C_2mpyr][FSI]), with a very wide plastic crystal phase range of −22 to 205 °C and good electrochemical stability was reported by Yoshizawa-Fujita et al.[9] However, [C_2mpyr][FSI] shows non-ideal mechanical properties at room temperature and at low levels of lithium addition a liquid phase is formed, which leads to a very soft quasi-solid material.

The preparation of composites has provided a new strategy for improving the mechanical and electrochemical properties for high-performance solid electrolyte materials.[10] For OIPCs, in particular, it has been shown that addition a small amount of SiO_2 nanoparticles into an OIPC (e.g., 1 to 10 wt% SiO_2 into *N*-ethyl-*N*-methylpyrrolidinium bis(trifluoromethanesulfonyl) amide) can increase the ionic conductivity due to an increase in defect size and concentration.[11] Recently, further progress has been made using a polymer nanofiber matrix prepared by electrospinning or co-electrospinning,[7b,12] which are easy to prepare and beneficial for the preparation of ultrathin flexible electrolyte membranes. It has also been shown that the interfacial interaction between the polymer surface and the OIPC constituent ions can induce expansion of the crystal lattice, which results in more defects in the OIPC/PVDF interfacial region and hence improved ionic conductivity.[12a]

Here, we demonstrate an alternative strategy to efficiently utilize these surface effects by coating an OIPC layer on commercial PVDF nanoparticles (**Figure 1**) and forming a dense composite material. Unlike the previously reported method utilizing electrospun nanofibers, here the as-synthesized composite electrolyte is composed of a majority weight fraction of PVDF particles and minority of OIPC. By simple coating of lithium doped [C_2mpyr][FSI] on the surface of PVDF nanoparticles, the obtained composite electrolyte exhibits greatly improved ion dynamics and enhanced ionic conductivity. The use of a majority of PVDF provides good mechanical integrity of the composite electrolyte—a key feature to improve battery safety during long-term cycling. Furthermore, the use of a commercial PVDF powder reduces the portion of relatively expensive OIPC component, allowing the preparation of a high-performance and low-cost solid composite electrolyte.

The OIPC-coated PVDF composite (OIPC/PVDF) was prepared by a simple coating and pressing method (Figure 1a). As shown in Figure 1b, at 30 °C the conductivity of $Li_{0.1}[C_2mpyr]_{0.9}[FSI]$/PVDF composites (subscript 0.1 and 0.9 represent the mole fraction of Li^+ and $[C_2mpyr]^+$ in the OIPC, respectively) increases slowly with loading content until 30 wt% $Li_{0.1}[C_2mpyr]_{0.9}[FSI]$, after which the conductivity increases significantly. Above 40 wt%, the conductivity decreases again, which is suggested to arise from the disconnection of the interfacial layer when the OIPC volume fraction exceeds the critical volume where all the interfacial pathways are connected. However, it is noteworthy that with OIPC loadings of 30–40 wt%, the conductivity of the OIPC/PVDF composite exceeds that of the $Li_{0.1}[C_2mpyr]_{0.9}[FSI]$ bulk material (red dashed line) (Figure 1b). There are two proposed effects to explain this increased conductivity. One is the percolation mechanism, which is normally described in conductive nanocomposite systems.[13] The other effect, which is the most important, may arise from the highly conductive layer coated on the surface of the PVDF particles (as supported by the NMR analysis, detailed further below). Additionally, it can be seen that with increased $Li_{0.1}[C_2mpyr]_{0.9}[FSI]$ loading, the pellet changes from white to transparent (inset of Figure 1b), suggesting improved coverage of the PVDF surface by the OIPC. A similar trend is apparent from the scanning electron microscopy (SEM) analysis (see Figure S1 in the Supporting Information); there are voids present in the composite when the OIPC loading is less than 40 wt%, showing insufficient coverage of the PVDF particles, while the composites with 40 and 50 wt% loading show a dense

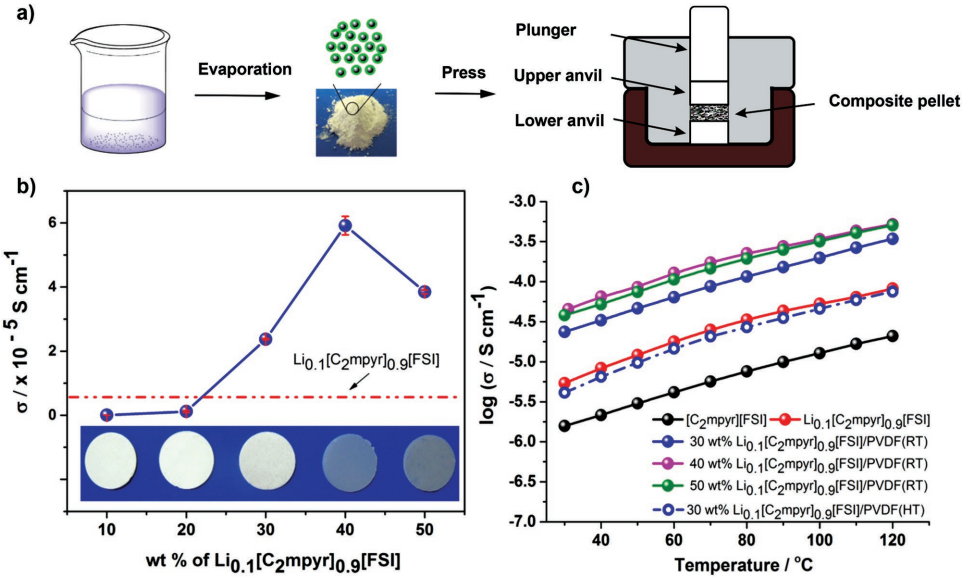

Figure 1. a) Schematic of the $Li_{0.1}[C_2mpyr]_{0.9}[FSI]$/PVDF composite electrolyte preparation procedure. b) The effect of $Li_{0.1}[C_2mpyr]_{0.9}[FSI]$ loading on the conductivity at 30 °C and (inset) the composite appearance, and c) the temperature dependence of the conductivity of the composite electrolytes. The wt% is the weight fraction of $Li_{0.1}[C_2mpyr]_{0.9}[FSI]$ in the total OIPC/PVDF composite. The room temperature pressed sample and the heat treated sample are labled as RT and HT, respectively.

structure with the voids filled by the OIPC. Assuming that there are minimal voids in the composite, this allows an estimate of the theoretical distribution of the PVDF particles within the OIPC matrix to be performed, which suggests an OIPC layer/coating thickness in the range of 20–30 nm for the 30 wt% system (Figure S1, Supporting Information).

It has been reported that heat treatment can effectively improve the mechanical stability and durability for polymeric matrix-based composites as a result of an interfacial "cross-linking" mechanism.[14] In our study, a heat treated (HT) composite was prepared, heated above the melting temperature of PVDF (see experimental section for preparation), which showed good flexibility and bendable properties (see Video in the Supporting Information), but suffered from a decreased conductivity (Figure 1c).

It has recently been reported that the interaction between PVDF and an OIPC can disrupt the ion packing in the OIPC, inducing a highly conductive amorphous phase at the interfacial region, resulting in enhanced ion dynamics and ionic conductivity.[12] Motional narrowing of the solid-state ^{7}Li-NMR line shape has often been used to probe the ion dynamics in solid electrolytes.[15] Therefore, to assess the impact of PVDF addition and the sample preparation history on the lithium ion dynamics in the composites, static ^{7}Li NMR spectra were measured (**Figure 2**a). The 30 wt% composite was selected for NMR analysis, from the range of non-heat treated samples, due to the dramatic conductivity change (Figure 1b). The heat treated composite, $Li_{0.1}[C_2mpyr]_{0.9}[FSI]$/PVDF(HT), exhibits a broader line in comparison to the bulk $Li_{0.1}[C_2mpyr]_{0.9}[FSI]$. The observed broadening can be understood in terms of the dipolar interaction between the PVDF and Li^+ in the $Li_{0.1}[C_2mpyr]_{0.9}[FSI]$/PVDF(HT), which would lead to slower lithium ion dynamics. Remarkably, the composite pressed at room temperature (labeled $Li_{0.1}[C_2mpyr]_{0.9}[FSI]$/PVDF (RT)) shows an even narrower line width than that of the bulk $Li_{0.1}[C_2mpyr]_{0.9}[FSI]$, suggesting significantly enhanced lithium ion dynamics after incorporation of the PVDF particles. This is consistent with the conductivity measurements (Figure 1b,c) which show that the 30 wt% $Li_{0.1}[C_2mpyr]_{0.9}[FSI]$/PVDF (RT) composites exhibit higher conductivity than the bulk $Li_{0.1}[C_2mpyr]_{0.9}[FSI]$.

To further understand the molecular level interactions between the Li^+ and the $[FSI]^-$ as well the PVDF chain, we measured the $^{19}F \rightarrow {}^{7}Li$ cross polarization (CP)-magic angle spinning (MAS) spectra (Figure 2b). Both the bulk $Li_{0.1}[C_2mpyr]_{0.9}[FSI]$ and the $Li_{0.1}[C_2mpyr]_{0.9}[FSI]$/PVDF (RT) show negligible NMR signal. Inefficient CP transfer between the ^{19}F and the ^{7}Li can be attributed to fast Li^+ and/or $[FSI]^-$ dynamics in the sample.

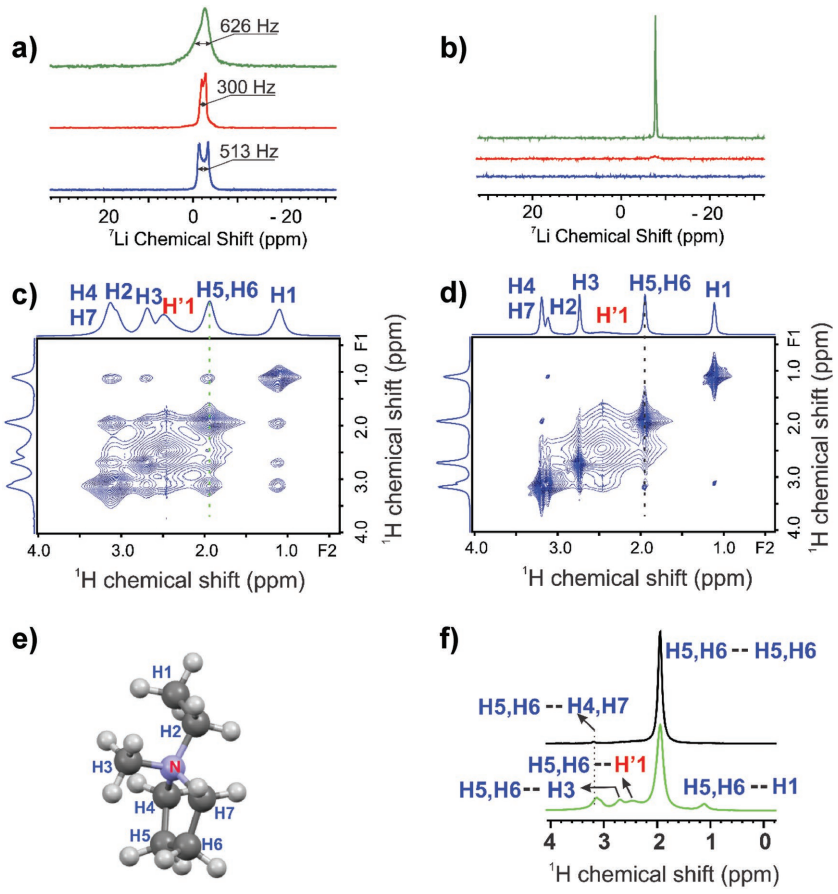

Figure 2. Solid-state NMR characterization of the composite electrolyte. a) ^{7}Li static NMR spectra of $Li_{0.1}[C_2mpyr]_{0.9}[FSI]$ (blue), 30 wt% $Li_{0.1}[C_2mpyr]_{0.9}[FSI]$/PVDF(RT) (red), 30 wt% $Li_{0.1}[C_2mpyr]_{0.9}[FSI]$/PVDF (HT) (green). b) $^{19}F \rightarrow {}^{7}Li$ cross polarization spectra of, $Li_{0.1}[C_2mpyr]_{0.9}[FSI]$ (blue), 30 wt% $Li_{0.1}[C_2mpyr]_{0.9}[FSI]$/PVDF(RT) (red), 30 wt% $Li_{0.1}[C_2mpyr]_{0.9}[FSI]$/PVDF(HT) (green). c,d) The NOESY spectra of the 30 wt% $Li_{0.1}[C_2mpyr]_{0.9}[FSI]$/PVDF(HT) and 30 wt% $Li_{0.1}[C_2mpyr]_{0.9}[FSI]$/PVDF(RT), respectively. H'1 represents the proton from the PVDF polymer chain. Both spectra intensities are normalized to the H1–H1 self-correlation peak as a unit, and both spectra are displayed with the same scale so that the intensities can be compared. e) The molecular structure and proton site annotation of the $[C_2mpyr]$ cation. f) 1D proton NMR slices at ≈1.9 ppm (H5, H6) taken from the NOESY spectra. The bottom and top spectra are sliced from c) and d), respectively.

In contrast, the $Li_{0.1}[C_2mpyr]_{0.9}[FSI]$/PVDF (HT) shows a substantial NMR signal, suggesting much slower ion dynamics, which is consistent with the static ^{7}Li NMR results in Figure 2a. Further 2D heteronuclear correlation experiments (Figure S2, Supporting Information) show that a strong interaction exists between Li^+ and $[FSI]^-$ in the $Li_{0.1}[C_2mpyr]_{0.9}[FSI]$/PVDF (HT) composite, whereas the interaction with the PVDF polymer chain is relatively weak.

As both the PVDF polymer and the $[C_2mpyr]^+$ cation contains protons, the interactions between the polymer chain and the OIPC cations can be analyzed using solid-state ^{1}H NMR techniques. Figure 2c,d shows the ^{1}H nuclear overhauser effect spectroscopy (NOESY) spectra of the composite samples prepared at RT and elevated temperature, respectively. Compared to the heat treated (HT) sample, $Li_{0.1}[C_2mpyr]_{0.9}[FSI]$/PVDF (RT) clearly shows narrower proton lines and lower cross-peak intensities, suggesting faster dynamics and weaker

homonuclear interactions. Further, a cross-peak between the H'1 from the PVDF and the H5, H6 sites of the $[C_2mpyr]^+$ cation can be clearly identified in the $Li_{0.1}[C_2mpyr]_{0.9}[FSI]$/PVDF (HT) sample (Figure 2c), which is not visible in the $Li_{0.1}[C_2mpyr]_{0.9}[FSI]$/PVDF (RT) sample. This feature can be more clearly seen from the 1D slices of the H5, H6 column taken from the NOESY spectra, which are shown in Figure 2f. This is strong evidence of molecular interaction between the PVDF molecules and the $[C_2mpyr]^+$ cations in the heat treated sample. Based on the NMR data and ionic conductivity behavior, it can be concluded that the coating of an OIPC layer on the PVDF particle surface generates a highly conductive phase with enhanced ion dynamics, especially high lithium mobility. With increased OIPC loading, once the highly conductive phase forms a continuous pathway for ion conduction (the threshold is ≈30% by weight in this study), a highly conductive solid-state electrolyte can be prepared. However, heat treatment at elevated temperature leads to significantly reduced dynamics of both the Li^+ and $[C_2mpyr]^+$, and subsequently reduced ionic conductivity (Figure 1c). This phenomenon can be explained by increased molecular interaction between the PVDF and the $[C_2mpyr]^+$ cations during heat treatment, which limits the ion mobility in the heat-treated composites.

As the 40 wt% $Li_{0.1}[C_2mpyr]_{0.9}[FSI]$/PVDF(RT) sample had enhanced Li^+ mobility and the highest ionic conductivity of all composite electrolytes prepared at room temperature, it was selected for further electrochemical investigation. The compatibility of the composite electrolyte with lithium metal, as well as the stability of the solid electrolyte interphase (SEI) layer, was evaluated by lithium|electrolyte|lithium symmetric cell cycling measurements at various current densities (0.1–0.5 mA cm^{-2}) at moderate temperatures (50 °C) and is shown in **Figure 3**a. To perform the preconditioning mechanism previously identified as beneficial for OIPC-based electrolytes,[7c,16] a 10 min charge–10 min discharge strategy was used initially. The cell polarization dropped from 750 mV for the first cycle to below 100 mV for the second cycle, after which it gradually decreased to a stable value. This preconditioning behavior is considered to arise from Joule heating effects and excess lithium dissolution near the electrolyte/electrode region, which can reduce the interfacial resistance.[16] The overpotential remained below 100 mV even at 0.5 mA cm^{-2} which, to the best of our knowledge, is the best performance reported for an OIPC system thus far.[16,17] The preconditioning behavior was further confirmed using impedance spectroscopy of a cell cycled at 0.2 mA cm^{-2} (Figure S4, Supporting Information). The interfacial resistance gradually decreased during the initial cycles and then increased slowly after the preconditioning process, which results from the growth of the SEI layer.[18] It is believed that the long-term cycling stability of the composite electrolyte is enabled by the wide electrochemical stability window (even wider than bulk $Li_{0.1}[C_2mpyr]_{0.9}[FSI]$, as shown in Figure S5, Supporting Information) and efficient lithium stripping and plating (Figure S6, Supporting Information).

Figure 3b,c shows the cycling performances of the $Li/LiFePO_4$ cells using 40 wt% $Li_{0.1}[C_2mpyr]_{0.9}[FSI]$/PVDF(RT) composite electrolytes. For the rate capability of the assembled $Li/LiFePO_4$ cell, a range of C rates from C/10 to 5 C was

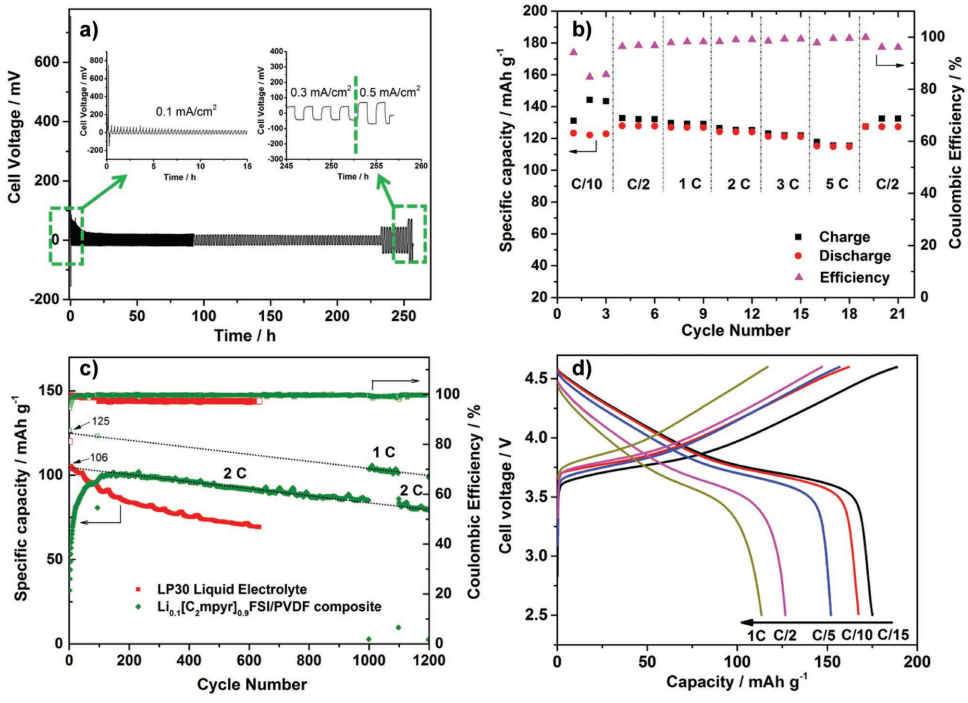

Figure 3. Electrochemical measurements of 40 wt% $Li_{0.1}[C_2mpyr]_{0.9}[FSI]$/PVDF(RT) composites. a) Symmetric cell cycling performance at various current densities, 50 °C. b) Specific capacities and Coulombic efficiencies of $Li/LiFePO_4$ cells at different current rates, ranging from C/10 to 5 C, 50 °C. c) Cycling stability of $Li/LiFePO_4$ cells at 2 C and room temperature (cut-off voltage 2.5–4.2 V). The cell consisting of commercial LP30 liquid electrolyte was used for comparison. d) Charge–discharge curves of the $Li/LiCo_{1/3}Ni_{1/3}Mn_{1/3}O_2$ cell using 40 wt% $Li_{0.1}[C_2mpyr]_{0.9}[FSI]$/PVDF(RT) composites (cut-off voltage 2.5–4.6 V), 50 °C.

used. During the first three cycles at C/10 (Figure 3b), a relatively low coulombic efficiency and discharge capacity (around 124 mAh g^{-1}) is observed, indicating irreversible SEI formation processes that have been reported previously.[19] However, the discharge capacity increases to 128 mAh g^{-1} at C/2 and then drops slightly from 127 mAh g^{-1} at 1 C to 124 mAh g^{-1} at 2 C and is even maintained at 115 mAh g^{-1} at 5 C. Additionally, the coulombic efficiency increases steadily from 96% at C/2 to 99% at 5 C, respectively.

To further test the long-term charge–discharge stability, a Li/$LiFePO_4$ cell with the composite electrolyte was cycled at a high current rate of 2 C at room temperature and 50 °C. As shown in Figure 3c, the coin cell with composite electrolyte shows very stable cycling performance: even after 1200 charge–discharge cycles at 2 C, the coulombic efficiency is maintained at 99.8%, much higher than the cell using LP30 electrolyte (efficiency of 97.3% after 630 cycles). For the cell cycled at 50 °C, as shown in Figure S10 (Supporting Information), after 100 cycles the cell still delivered a capacity of 119 mAh g^{-1}, with capacity retention of 90% and decay rate of 0.13 mAh g^{-1} per cycle. By contrast, the Li/$LiFePO_4$ cell cycled under the same conditions with commercial LP30 liquid electrolyte shows an obvious decay (0.48 mAh g^{-1} per cycle) with capacity retention of 64% after 100 cycles. The improved cycling stability of the composite electrolyte can be ascribed to the formation of a stable SEI layer and less increase in charge transfer resistance compared with the liquid electrolyte during charge–discharge (Figure S9, Supporting Information). To the best of our knowledge, this is the first demonstration of long-term cycling performance at such high rates for an OIPC-based electrolyte, and the results are comparable to the performance of ionic liquid systems.[20]

Prompted by the high oxidation stability of 40 wt% $Li_{0.1}[C_2mpyr]_{0.9}[FSI]$/PVDF(RT) electrolyte (Figure S7, Supporting Information), we further investigated the battery charge–discharge performance with another high voltage cathode material, $LiCo_{1/3}Ni_{1/3}Mn_{1/3}O_2$ (LiNMC), chosen for its high capacity and low cost.[21] As shown in Figure 3d and Figure S8 (Supporting Information), the assembled coin cell was charged and discharged between 2.5 and 4.6 V at 50 °C under different rates (C rates), ranging from C/15 to 1 C. The discharge capacities obtained at C/15 and 1 C are 178 and 113 mAh g^{-1}, respectively. Although the rate of capacity fade was more pronounced for these cells (compared to the $LiFePO_4$ cells), this result still indicates that these composite electrolytes have promise for application with high voltage cathodes for high energy density, all-solid-state lithium battery applications.

In summary, a highly conductive solid electrolyte has been prepared using a facile procedure by simple pressing of OIPC-coated PVDF particles. The use of commercial PVDF powder not only acts as mechanical support but, most importantly, can induce a more conductive layer at the interface between the OIPC and the PVDF. Thus, highly conductive channels with improved ion dynamics can be easily produced in the OIPC/PVDF composites. The ionic conductivity of the as-prepared composite is significantly improved using only 40 wt% of Li-OIPC incorporated with commercial PVDF powder, achieving ≈10^{-4} S cm^{-1} at room temperature. When evaluated in lithium symmetric cells, the composite shows stable cycling at different current densities, ranging from 0.1 to 0.3 mA cm^{-2}, which is one of the best results reported thus far for solid state OIPC-based electrolytes. The cells using a $LiFePO_4$ electrode and 40 wt% $Li_{0.1}[C_2mpyr]_{0.9}[FSI]$/PVDF composite electrolyte exhibit high specific capacity (119 mAh g^{-1} at 2 C after 100 cycles and 0.13 mAh g^{-1} per cycle decay rate at 50 °C) and high cycling stability (coulombic efficiency of 99.8% after 1200 cycles at 2 C, room temperature). The composite electrolyte was further tested with LiNMC electrode and considerable capacities have been achieved (178 and 113 mAh g^{-1} at C/15 and 1 C, respectively). The low weight fraction of OIPC, excellent electrochemical stability as well as solid properties of the novel composite electrolytes prepared via this strategy provide a promising new pathway for the development of low cost, high energy density, and safer all solid-state lithium metal batteries.

Experimental Section

Preparation of $Li_{0.1}[C_2mpyr]_{0.9}[FSI]$/PVDF Composite Electrolyte: The organic ionic plastic crystal, $[C_2mpyr][FSI]$, was synthesized following the previously reported method.[9] Commercial PVDF powder (Sigma-Aldrich, batch No. 140317) was dried in a vacuum oven overnight at 50 °C before use. Lithium bis(fluorosulfonyl)amide (LiFSI) was purchased from Coorstek and used as received.

For the preparation of $Li_{0.1}[C_2mpyr]_{0.9}[FSI]$/PVDF composite electrolytes, LiFSI and $[C_2mpyr][FSI]$ (mole ratio 1: 9) were dissolved in methanol and stirred for 1 h at room temperature to obtain a clear solution. Then a known amount of PVDF powder was added into the solution and the mixture stirred for 2 h to obtain a slurry. The $Li_{0.1}[C_2mpyr]_{0.9}[FSI]$-coated PVDF powder samples were subsequently prepared by quick evaporation of the solvent by flushing with dry N_2 gas. After solvent evaporation, the obtained white powder was carefully ground with an agate mortar and pestle and dried under vacuum at 50 °C for at least 12 h before use.

For the preparation of composite pellets, $Li_{0.1}[C_2mpyr]_{0.9}[FSI]$/PVDF powder (60–80 mg) was added into a KBr die in an Argon-filled glove box and pressed at room temperature under 4 tons of hydrostatic pressure. The thickness of the pressed pellet was ≈220 µm (±5%). To investigate the effects of heat treatment on the composite electrolyte properties, the KBr die together with powder were heated in a vacuum oven at 185 °C (≈20 °C higher than melting point of PVDF) for 30 min and then quickly pressed using the same pressure above. The pressed samples were then dried under vacuum at 50 °C before further characterization.

Solid-State NMR: All the solid-state NMR measurements were performed on a Bruker 500M Widebore NMR spectrometer. Samples were packed into 4 mm or 2.5 mm ZrO_2 MAS rotors in an argon-filled glove box. Both the ^7Li static NMR and the $^{19}F \rightarrow {}^7Li$ CPMAS spectra were recorded using a 4 mm H/F-X double resonance MAS probe. For CPMAS experiments, the MAS rate was 10 kHz, recycle delay was 2 s and 8192 scans were accumulated for all samples. ^1H NOESY spectra were measured with a 2.5 mm H/F-X double resonance MAS probe. The mixing time was 10 ms, MAS rate was 25 kHz and the recycle delay was 2 s for both samples. The ^7Li chemical shifts were referenced using 0.1 M LiCl/H_2O solution (δ_{Li} = 0 ppm). The ^1H and ^{13}C chemical shifts were calibrated using adamantane as the reference (δ_H = 1.63 ppm, δ_{CH2} = 29.5 ppm).

Electrochemical Characterization: The ionic conductivity of the composite electrolytes was measured by electrochemical impedance spectroscopy using a Solartron Modulab (Solartron Analytical, Ametek) according to our previously reported procedures.[12b] For each sample, two heating scans and one cooling scan were performed and the reported data were collected during the second heating scan.

Lithium metal symmetric cells were prepared in order to evaluate the lithium metal/composite electrolyte compatibility and cycling stability at 50 °C. First, the lithium strips (Sigma Aldrich) were brushed and punched into lithium discs (8 mm in diameter) and the composite

electrolyte was sandwiched between two lithium discs and assembled into a coin cell. These preparations were all performed in an argon-filled glove box. The symmetric cells were cycled using a Bio-Logic VMP3/Z potentiostat controlled by EC-lab (version 10.44) at 50 °C.

Two active materials, $LiFePO_4$ (Phostech) and $Li(Ni_{1/3}Co_{1/3}Mn_{1/3})O_2$ (LiNMC, Targray Technology International Inc.), were used for the battery performance test. The cathode films were prepared by painting a mixture of active material, C65 (Imerys Graphite & Carbon) and PVDF binder (Sigma Aldrich) onto Al foil. *N*-methyl-2-pyrrolidone (Sigma-Aldrich) was used as the solvent and the ratio of active material, C65, PVDF was 80:10:10 and 85:10:5 for $LiFePO_4$ and LiNMC cathode, respectively. Cathode discs (8 mm in diameter with active material loading of 1.2–1.5 mg cm^{-2}) were punched out and dried in a vacuum oven before use. The anode was prepared using the same method described in the symmetric cell preparation section. During coin cell assembly, melted OIPC (≈5 µL) was applied to the electrode surface to improve the electrode/electrolyte contact and ion transport. $Li/LiFePO_4$ cells were cycled at room temperature and 50 °C, respectively. For comparison, coin cells consisting of LP30 liquid electrolyte (1 M $LiPF_6$ in ethylene carbonate/dimethyl carbonate, 1:1 by volume, Solvionic) and Celgard polyethylene separator were also assembled and tested at same conditions. $Li/Li(Ni_{1/3}Co_{1/3}Mn_{1/3})O_2$ cells were cycled at 50 °C. For the tests at 50 °C, all the cells were placed in a 50 °C oven and cycled using a Bio-Logic VMP3/Z potentiostat controlled by EC-lab (version 10.44).

Supporting Information

Supporting Information is available from the Wiley Online Library or from the author.

Acknowledgements

This work was financially supported by Australian Research Council (ARC) through the ARC Discovery Program (DP140101535). Prof. M.F. is grateful to the support of Australian Laureate Fellowship (FL110100013). Dr. G.W.G acknowledges support from the ARC through a Discovery Early Career Research Award (DE130101458). The authors also thank Dr. Nicolas Goujon for the preparation of the $LiFePO_4$ cathode film.

Conflict of Interest

The authors declare no conflict of interest.

Keywords

composite electrolytes, lithium metal batteries, organic ionic plastic crystals, solid state NMR

Received: February 22, 2017
Revised: March 5, 2017
Published online:

[1] a) J. Kalhoff, G. G. Eshetu, D. Bresser, S. Passerini, *ChemSusChem* **2015**, *8*, 2154; b) L. Long, S. Wang, M. Xiao, Y. Meng, *J. Mater. Chem. A* **2016**, *4*, 10038.

[2] a) R. P. Doyle, X. Chen, M. Macrae, A. Srungavarapu, L. J. Smith, M. Gopinadhan, C. O. Osuji, S. Granados-Focil, *Macromolecules* **2014**, *47*, 3401; b) S. Chen, F. Dai, M. L. Gordin, Z. Yu, Y. Gao, J. Song, D. Wang, *Angew. Chem. Int. Ed.* **2016**, *55*, 4231; c) R. Meziane, J.-P. Bonnet, M. Courty, K. Djellab, M. Armand, *Electrochim. Acta* **2011**, *57*, 14.

[3] I. Osada, H. de Vries, B. Scrosati, S. Passerini, *Angew. Chem. Int. Ed.* **2016**, *55*, 500.

[4] a) R. He, T. Kyu, *Macromolecules* **2016**, *49*, 5637; b) M. S. Michael, M. M. E. Jacob, S. R. S. Prabaharan, S. Radhakrishna, *Solid State Ionics* **1997**, *98*, 167.

[5] V. Thangadurai, S. Narayanan, D. Pinzaru, *Chem. Soc. Rev.* **2014**, *43*, 4714.

[6] a) D. R. MacFarlane, J. Huang, M. Forsyth, *Nature* **1999**, *402*, 792; b) J. M. Pringle, *Phys. Chem. Chem. Phys.* **2013**, *15*, 1339; c) V. Armel, D. Velayutham, J. Sun, P. C. Howlett, M. Forsyth, D. R. MacFarlane, J. M. Pringle, *J. Mater. Chem.* **2011**, *21*, 7640.

[7] a) V. Armel, M. Forsyth, D. R. MacFarlane, J. M. Pringle, *Energy Environ. Sci.* **2011**, *4*, 2234; b) P. C. Howlett, F. Ponzio, J. Fang, T. Lin, L. Jin, N. Iranipour, J. Efthimiadis, *Phys. Chem. Chem. Phys.* **2013**, *15*, 13784; c) P. C. Howlett, Y. Shekibi, D. R. MacFarlane, M. Forsyth, *Adv. Eng. Mater.* **2009**, *11*, 1044; d) L. Y. Jin, P. Howlett, J. Efthimiadis, M. Kar, D. R. Macfarlane, M. Forsyth, *J. Mater. Chem.* **2011**, *21*, 10171; e) U. A. Rana, M. Forsyth, D. R. MacFarlane, J. M. Pringle, *Electrochim. Acta* **2012**, *84*, 213.

[8] L. Jin, K. M. Nairn, C. M. Forsyth, A. J. Seeber, D. R. MacFarlane, P. C. Howlett, M. Forsyth, J. M. Pringle, *J. Am. Chem. Soc.* **2012**, *134*, 9688.

[9] M. Yoshizawa-Fujita, E. Kishi, M. Suematsu, T. Takekawa, M. Rikukawa, *Chem. Lett.* **2014**, *43*, 1909.

[10] a) F. Croce, G. B. Appetecchi, L. Persi, B. Scrosati, *Nature* **1998**, *394*, 456; b) F. Croce, L. Persi, F. Ronci, B. Scrosati, *Solid State Ionics* **2000**, *135*, 47.

[11] Y. Shekibi, A. Gray-Weale, D. R. MacFarlane, A. J. Hill, M. Forsyth, *J. Phys. Chem. C* **2007**, *111*, 11463.

[12] a) N. Iranipour, D. J. Gunzelmann, A. Seeber, J. Vongsvivut, C. Doherty, F. Ponzio, L. A. O'Dell, A. F. Hollenkamp, M. Forsyth, P. C. Howlett, *J. Mater. Chem. A* **2015**, *3*, 6038; b) X. Wang, H. Zhu, G. W. Greene, J. Li, N. Iranipour, C. Garnier, J. Fang, M. Armand, M. Forsyth, J. M. Pringle, P. C. Howlett, *J. Mater. Chem. A* **2016**, *4*, 9873.

[13] M. A. S. Azizi Samir, F. Alloin, W. Gorecki, J.-Y. Sanchez, A. Dufresne, *J. Phys. Chem. B* **2004**, *108*, 10845.

[14] a) X. Wang, H. Tang, M. Pan, *J. Membr. Sci.* **2011**, *379*, 106; b) H. Tang, M. Pan, F. Wang, P. K. Shen, S. P. Jiang, *J. Phys. Chem. B* **2007**, *111*, 8684.

[15] G. W. Greene, F. Ponzio, N. Iranipour, H. Zhu, A. Seeber, M. Forsyth, P. C. Howlett, *Electrochim. Acta* **2015**, *175*, 214

[16] L. Jin, P. C. Howlett, J. Efthimiadis, M. Kar, D. MacFarlane, M. Forsyth, *J. Mater. Chem.* **2011**, *21*, 10171.

[17] P. C. Howlett, J. Sunarso, Y. Shekibi, E. Wasser, L. Jin, D. R. MacFarlane, M. Forsyth, *Solid State Ionics* **2011**, *73*, 204.

[18] A. Manuel Stephan, K. S. Nahm, *Polymer* **2006**, *47*, 5952.

[19] L. Jin, P. C. Howlett, J. M. Pringle, J. Janikowski, M. Armand, D. R. MacFarlane, M. Forsyth, *Energy Environ. Sci.* **2014**, *7*, 3352.

[20] H. Yoon, G. H. Lane, Y. Shekibi, P. C. Howlett, M. Forsyth, A. S. Best, D. R. MacFarlane, *Energy Environ. Sci.* **2013**, *6*, 979.

[21] K. M. Shaju, P. G. Bruce, *Adv. Mater.* **2006**, *18*, 2330.